THE JOURNAL OF BIOLOGICAL CHEMISTRY
Vol. 279, No. 15, Issue of April 9, pp. 15541–15549, 2004
Printed in U.S.A.

Cell Surface Expression of α_{1D}-Adrenergic Receptors Is Controlled by Heterodimerization with α_{1B}-Adrenergic Receptors*

Received for publication, December 22, 2003, and in revised form, January 12, 2004
Published, JBC Papers in Press, January 21, 2004, DOI 10.1074/jbc.M314014200

Chris Hague‡, Michelle A. Uberti, Zhongjian Chen, Randy A. Hall§, and Kenneth P. Minneman¶

From the Department of Pharmacology, Emory University, Atlanta, Georgia 30322

α_1-Adrenergic receptors (ARs) belong to the large Class I G protein-coupled receptor superfamily and comprise three subtypes (α_{1A}, α_{1B}, and α_{1D}). Previous work with heterologously expressed C-terminal green fluorescent protein (GFP)-tagged α_1-ARs showed that α_{1A}- and α_{1B}-ARs localize to the plasma membrane, whereas α_{1D}-ARs accumulate intracellularly. We recently showed that α_{1D}- and α_{1B}-ARs form heterodimers, whereas α_{1D}- and α_{1A}-ARs do not. Here, we examined the role of heterodimerization in regulating α_{1D}-AR localization using both confocal imaging of GFP- or CFP-tagged α_1-ARs and a luminometer-based surface expression assay in HEK293 cells. Co-expression with α_{1B}-ARs caused α_{1D}-ARs to quantitatively translocate to the cell surface, but co-expression with α_{1A}-ARs did not. Truncation of the α_{1B}-AR extracellular N terminus or intracellular C terminus had no effect on surface expression of α_{1D}-ARs, suggesting primary involvement of the hydrophobic core. Co-transfection with an uncoupled mutant α_{1B}-AR ($\Delta 12\alpha_{1B}$) increased both α_{1D}-AR surface expression and coupling to norepinephrine-stimulated Ca^{2+} mobilization. Finally, GFP-tagged α_{1D}-ARs were not detected on the cell surface when expressed in rat aortic smooth muscle cells that express no endogenous ARs, but were almost exclusively localized on the surface when expressed in DDT$_1$MF-2 cells, which express endogenous α_{1B}-ARs. These studies demonstrate that α_{1B}/α_{1D}-AR heterodimerization controls surface expression and functional coupling of α_{1D}-ARs, the N- and C-terminal domains are not involved in this interaction, and that α_{1B}-AR G protein coupling is not required. These observations may be relevant to many other Class I G protein-coupled receptors, where the functional consequences of heterodimerization are still poorly understood.

α_1-Adrenergic receptors (ARs)[1] belong to the rhodopsin-like Class I G protein-coupled receptor (GPCR) family (1). There are three closely related α_1-AR subtypes (α_{1A}, α_{1B}, and α_{1D}) with similar pharmacological and signaling properties. Activation of each subtype stimulates phospholipase C, release of intracellular Ca^{2+}, and activation of mitogenic pathways (2–4). Generation of both single (5–7) and double (8) α_1-AR knock-out mice has shown that all three subtypes contribute to overall control of blood pressure. Although recent reports suggest that α_1-ARs cause different transcriptional responses (9) or differentially interact with other proteins (10–12), functional differences between these closely related receptors remain unclear.

To date, the clearest differences between α_1-AR subtypes are in their subcellular localizations. Confocal imaging of GFP-tagged α_1-ARs has shown that heterologously expressed α_{1A}- and α_{1B}-ARs are found primarily at the plasma membrane, whereas α_{1D}-ARs accumulate intracellularly in a variety of cell lines (13, 14). Similar conclusions were made for native receptors using fluorescent ligands for localization in animal tissues (15). Interestingly, membrane expression correlates with differences in coupling efficiencies for α_1-AR subtypes ($\alpha_{1A} > \alpha_{1B} \geq \alpha_{1D}$) in transfected cells (13–18) but does not predict responses *in vivo*. α_{1D}-ARs mediate contractile responses to catecholamines in several blood vessels (19–21) with high potencies and intrinsic activities. We reported previously that N-terminal truncation increased α_{1D}-AR binding, functional responses, and surface membrane expression (17, 18), but there is no evidence that α_{1D}-ARs are N-truncated *in viv*o. It seems more likely that difficulties in heterologous expression of α_{1D}-ARs relate to the lack of accessory trafficking proteins.

There are now many reports of homo- and hetero-dimerization of GPCRs (22–27). In fact, it now appears that the *majority* of GPCRs can form dimers, often with distantly related receptors (28–33). However, with the exception of Class III $GABA_B$ (34) and taste receptors (35), where hetero-oligomerization is required to form a single functional receptor, GPCR dimerization only rarely results in clearly observable changes in pharmacology or functional responses. Thus the functional significance of Class I GPCR dimerization remains a matter of active debate.

We previously reported that epitope-tagged α_1-ARs exist as both monomers and dimers (36). Heterodimerization between these receptors has now been widely reported (37–39). We found in previous studies that α_1-AR heterodimerization is subtype-specific, with α_{1B}-ARs interacting with α_{1A}- or α_{1D}-ARs, but with no detectable interactions between α_{1A}- and α_{1D}-ARs (39). Interestingly, heterodimerization did not alter apparent ligand-binding properties but, rather, resulted in increased receptor expression (39). In particular, α_{1B}/α_{1D}-AR heterodimerization increased surface expression of α_{1D}-ARs as

* The costs of publication of this article were defrayed in part by the payment of page charges. This article must therefore be hereby marked "*advertisement*" in accordance with 18 U.S.C. Section 1734 solely to indicate this fact.

§ Supported by grants from the National Institutes of Health (NIH) and by a Distinguished Young Scholar in Medical Research Award from the W.M. Keck Foundation.

¶ Supported by grants from the NIH.

‡ To whom correspondence should be addressed: Dept. of Pharmacology, Emory University, Atlanta, GA 30322. Tel.: 404-727-0363; Fax: 404-727-0365; E-mail: chague@emory.edu.

[1] The abbreviations used are: AR, adrenergic receptor; GPCR, G protein-coupled receptor; GFP, green fluorescent protein; CFP, cyan fluorescent protein; NE, norepinephrine; RASM, rat aortic smooth muscle; HEK, human embryonic kidney; HA, hemagglutinin; PBS, phosphate-buffered saline; PBS+, PBS plus 0.5% horse serum; HRP, horseradish peroxidase; ECL, enhanced chemiluminescence; BSA, bovine serum albumin; DMEM, Dulbecco's modified Eagle's medium; InsP, inositol phosphate; BSS, biological salt solution; CMV, cytomegalovirus; $GABA_B$, γ-aminobutyric acid, type B; fura-2/AM, fura-2/acetoxymethylester; ER, endoplasmic reticulum.

monitored by a luminometer assay (39). From these data, we hypothesized that α_{1B}/α_{1D}-AR heterodimerization might help traffic α_{1D}-ARs to the plasma membrane where they would be accessible to their hydrophilic ligands.

In this study, we used a combination of N- and C-terminally tagged α_1-ARs to investigate the role of α_1-AR dimerization in regulating receptor localization and function. We found that co-expression of α_{1B}/α_{1D}-AR heterodimers quantitatively promotes surface expression of α_{1D}-ARs and also increases coupling to intracellular Ca^{2+} release. This interaction is subtype-specific, does not require the N- or C-terminal domains of the receptor, and is not dependent on α_{1B}-AR G protein coupling. These data provide a clear example of the physiological importance of heterodimerization for a Class I GPCR subtype, the α_{1D}-AR, which has been difficult to study functionally due to its predominantly intracellular localization when expressed alone in many cell types.

EXPERIMENTAL PROCEDURES

Materials—Materials were obtained from the following sources: cDNAs for the wild type human α_{1A}-AR (40), and human α_{1A}-, α_{1B}-, and α_{1D}-AR C-terminally tagged GFP constructs in pEGFP-N3 (12, 13) were generously provided by Dr. Gozoh Tsujimoto (National Children's Hospital, Tokyo, Japan), human α_{1B}-AR cDNA (41) was a gift from Dr. Dianne Perez (Cleveland Clinic, Cleveland, OH), human α_{1D}-AR cDNA was cloned in our laboratory (42); pECFP-N1 vector was a gift from Dr. John Hepler (Emory University, Atlanta, GA); hamster α_{1B}-AR and $\Delta12\alpha_{1B}$-AR in pCMV were a gift from Dr. Myron Toews (University of Nebraska Medical Center, Omaha, NE); rat aortic smooth muscle (RASM) cells were a gift from Dr. T. J. Murphy (Emory University, Atlanta, GA); fura-2/acetoxymethylester (fura-2/AM) and *n*-dodecyl-β-D-maltoside were purchased from Calbiochem (La Jolla, CA); HEK293, DDT_1MF-2, and Phoenix producer cells from ATCC (Manassas, VA); (−)-norepinephrine bitartrate, Dowex-1 resin, HRP-conjugated anti-FLAG M2 antibody, Dulbecco's modified Eagle's medium (DMEM), bovine serum albumin (BSA), penicillin, and streptomycin from Sigma Chemical Co. (St. Louis, MO); *myo*-[^{3}H]inositol from American Radiolabeled Chemicals Inc. (St. Louis, MO); SuperFect transfection reagent from Qiagen (Valencia, CA); enzyme-linked immunosorbent assay ECL from Pierce (Rockford, IL); Vectashield mounting medium from Vector Laboratories (Burlingame, CA); and anti-HA polyclonal antibody and Texas Red conjugated anti-rabbit antibody from Clontech (Palo Alto, CA).

Construction of Tagged and Truncated α_1-ARs—Human α_1-AR cDNAs were subcloned into the mammalian expression vector pDT containing in-frame N-terminal hexahistidine and FLAG epitope tags as previously described (36, 39). After sequencing, unique restriction sites were used to replace the FLAG-hexahistidine tag in pDT with the HA-epitope tag using complementary annealed oligonucleotides with appropriate overhangs. N-terminally truncated human α_{1B}-ARs ($\Delta^{1-38\alpha1B}$) were generated by PCR using specific primers on human α_{1B}-AR cDNA in pDT, subcloned, and sequenced. C-terminal truncated α_{1B}-ARs ($\Delta^{366-519}\alpha_{1B}$) were generated using PCR to insert a stop codon ~20 amino acids after the predicted seventh transmembrane domain at the conserved glutamine at position 366. To create CFP-tagged α_{1A}-AR, α_{1B}-AR and α_{1D}-ARs, the pECFP-N1 vector was modified by removing one nucleotide (C^{667}). In brief, pECFP-N1 was digested with KpnI and AgeI, gel-extracted, and annealed to a double-stranded linker oligonucleotide with appropriate overhangs (forward: CGCCGGGCCGGGATCCA; reverse: CCGGTGGATCCCGGCCCGCGGTAC), minus the cytosine at position 667. The absence of C^{667} resulted in destruction of the ApaI restriction site, which was used as a diagnostic test. α_{1A}-, α_{1B}-, and α_{1D}-AR coding sequences were then cut from pEGFP-N3 using EcoRI and KpnI, gel-extracted, and ligated into the modified pECFP-N1 vector in-frame with the CFP tag.

Cell Culture and Transfection—HEK293, DDT_1MF-2, and RASM cells were propagated in DMEM with sodium pyruvate supplemented with 10% heat-inactivated fetal bovine serum, 100 μg/ml streptomycin, and 100 units/ml penicillin at 37 °C in a humidified atmosphere with 5% CO_2. Confluent plates were subcultured at a ratio of 1:5 for transfection. HEK293 and DDT_1MF-2 cells were transfected with 10 μg of DNA of each construct for 3 h using SuperFect® transfection reagent, and cells were used for experimentation 48–72 h after transfection. Because of the extremely low plasmid transfection efficiency, RASMs were transfected with infectious retroviral supernatants harvested from transfected Phoenix producer cells generated by a helper virus-free protocol as described previously (43).

Luminometer Based Surface Expression Assay—HEK293 cells were transiently transfected with FLAG- or HA-N-terminal-tagged human α_1-AR subtypes with SuperFect® for 24 h. Cells were split into poly-D-lysine-coated 35-mm dishes and grown overnight at 37 °C. Cells were then rinsed 3× with phosphate-buffered saline (PBS), fixed with 2% paraformaldehyde in PBS for 30 min, and rinsed 3× with PBS. Cells were then incubated in blocking buffer (2% nonfat milk in PBS, pH 7.4) for 30 min, and then incubated with the appropriate concentrations of HRP-conjugated M2-anti-FLAG or HRP-conjugated anti-HA antibody in blocking buffer for 1 h at room temperature. Cells were washed 3× with blocking buffer, 1× with PBS, and then incubated with enzyme-linked immunosorbent assay ECL reagent (Pierce) for 15 s. Luminescence was determined using a TD20/20 luminometer (Turner Designs, Sunnyvale, CA). For internalization assays, cells were first rinsed and then stimulated with or without 100 μM norepinephrine (NE) in DMEM for 1 h before the above procedure. Mean values ± S.E. were calculated as percent absorbance in arbitrary units and statistically compared using the unpaired *t* test, with a *p* value less then 0.05 considered significant.

Laser Confocal Microscopy—Cells transiently transfected with HA-, CFP-, or GFP-tagged constructs were grown on sterile coverslips, fixed for 30 min with 2% paraformaldehyde in 0.1 M phosphate buffer, pH 7.4, and rinsed 3× with PBS containing 0.5% normal horse serum (PBS+). For anti-HA immunostaining, fixed coverslips were blocked for 1 h in blocking buffer (PBS containing 1% BSA, 5% normal horse serum) containing 0.01% Triton X-100 to permeabilize cells. Anti-HA antibody was added to coverslips overnight at 4 °C at 1:500 dilution in blocking buffer, washed 3× with PBS+, and incubated with Texas Red-conjugated anti-rabbit IgG secondary antibody for 1 h at room temperature at 1:500 dilution in blocking buffer. Coverslips were washed 3× with PBS+ and mounted onto slides using Vectashield mounting medium. Cells were scanned with a Zeiss LSM 510 laser scanning confocal microscope (Heidelberg, Germany) as described previously (44). For detecting GFP and CFP, fluorescein isothiocyanate fluorescence was excited using an argon laser at a wavelength of 488 nm, and the absorbed wavelength was detected for 510–520 nm for GFP and 480–490 nm for CFP. For detecting Texas Red, rhodamine fluorescence was excited using a helium-neon laser at a wavelength of 522 nm. The pinhole size was maintained at 1 airy unit for all images.

Measurement of Ca^{2+} Mobilization—Intracellular Ca^{2+} mobilization was measured after preloading with fura-2 as described previously (16). In brief, confluent 150-mm plates of transiently transfected HEK293 cells were washed with biological salt solution (BSS) (in mM: NaCl, 130; KCl, 5; $MgCl_2$, 1; $CaCl_2$, 1.5; HEPES, 20; glucose, 10; with 0.1% BSA), gently detached using trypsin in Ca^{2+}-free Hanks' solution, and centrifuged for 2 min at 1000 × *g* at 4 °C. Cells were resuspended in DMEM containing 0.05% BSA and incubated with 1 μM fura-2/AM for 15 min at 37 °C. Cells were then diluted, centrifuged, and resuspended into 3-ml aliquots (2.0×10^6 cells/ml) and placed on ice. Prior to use, cells were warmed to 37 °C, pelleted at 1000 × *g* for 2 min, resuspended in 3 ml of BSS, transferred to a cuvette, and placed in a PerkinElmer Life Sciences LS50 luminescence spectrofluorometer (Beaconsfield, Buckingshamshire, UK). Excitation wavelengths were 340 and 380 nm, and the emission wavelength was 510 nm. Calculation of $[Ca^{2+}]_i$ was performed by equilibrating intra- and extracellular Ca^{2+} with 30 μM digitonin (R_{max}) followed by addition of 9 mM EGTA, 1 M Tris, pH 9.0 (R_{min}), and using a K_D of 225 nM for fura-2. 100 μM NE was used to stimulate α_1-AR-induced Ca^{2+} mobilization and was normalized to $[Ca^{2+}]_i$ stimulated by 100 μM UTP. Mean values ± S.E. were calculated and were statistically compared using the unpaired *t* test, with a *p* value less then 0.05 considered significant.

Measurement of [^{3}H]InsP Formation—Accumulation of [^{3}H]inositol phosphates (InsPs) was determined in confluent 96-well plates. Transiently transfected HEK293 cells were prelabeled with *myo*-[^{3}H]inositol for 48 h, and production of [^{3}H]InsP was determined by modification of a protocol described previously (45). After prelabeling, medium containing *myo*-[^{3}H]inositol was removed, and 100 μl of Krebs Ringer bicarbonate buffer (in mM: NaCl, 120; KCl, 5.5; $CaCl_2$, 2.5; NaH_2PO_4, 1.2; $MgCl_2$, 1.2; $NaHCO_3$, 20; glucose, 11; Na_2EDTA, 0.029) containing 10 mM LiCl was gently added to each well. Cells were incubated with or without 100 μM NE for 60 min. The reaction was stopped by addition of 100 μl of 20 mM formic acid, and samples were sonicated for 10 s. Samples were subjected to anion exchange chromatography to isolate [^{3}H]InsPs, which were quantified by scintillation counting. Total [^{3}H]-inositol incorporation in each sample was determined by removing 5-μl

aliquots prior to chromatography and counting. Percent hydrolysis of total *myo*-[^{3}H]inositol into [^{3}H]InsPs was calculated as cpm of [^{3}H]InsP divided by total cpm of [^{3}H]inositol incorporated, and expressed as mean ± S.E. Mean values were compared using the unpaired *t* test, with a *p* value less then 0.05 considered significant.

RESULTS

Cellular Localization of α_1-AR Subtypes—To provide an overview of the subcellular localization patterns of individually expressed α_1-AR subtypes, α_1-ARs tagged at the C terminus with either GFP or CFP were transiently transfected into HEK293 cells, fixed on coverslips, and examined using confocal microscopy. As shown in Fig. 1 and Table I, both GFP- and CFP-tagged α_{1A}- and α_{1B}-ARs were primarily located at the plasma membrane, whereas α_{1D}-ARs showed almost exclusively intracellular localization, as reported previously (13, 18).

α_{1B}-/α_{1D}-AR Heterodimerization Quantitatively Promotes Surface Expression of α_{1D}-ARs—Previously, we found that epitope-tagged α_{1B}- and α_{1D}-ARs co-immunoprecipitate following co-expression in HEK293 cells (39). To examine the effect of α_{1B}-/α_{1D}-AR heterodimerization on cellular localization, HEK293 cells were co-transfected with GFP-tagged α_{1D}-ARs and HA-tagged α_{1B}-ARs, or with GFP-tagged α_{1B}-ARs and CFP-tagged α_{1D}-ARs. As shown in Fig. 2*A*, confocal imaging of fixed cells demonstrated that co-expression of α_{1B}- and α_{1D}-ARs resulted in complete translocation of α_{1D}-ARs from intracellular sites to the plasma membrane. This was observed in all cells that expressed both constructs (data not shown). To study this using a different technique, HEK293 cells were co-transfected with FLAG-tagged α_{1D}-ARs and HA-tagged α_{1B}-ARs, and cell surface expression of FLAG-α_{1D}-ARs was quantified using a luminometer-based assay (Fig. 2*C*). In comparison to transient expression of α_{1D}-ARs alone, co-expression of α_{1B}- with α_{1D}-ARs resulted in a significant increase (6.7-fold) in α_{1D}-AR cell surface expression, which is strikingly similar to the -fold increase (6.6-fold) in α_{1D}-AR cell surface expression observed with cell counts (Table I). Because the cell counts were performed only with GFP fluorescence, we could not distinguish cells that expressed only one receptor subtype from those that expressed both, probably accounting for the only partial α_{1D}-AR translocation. These data clearly demonstrate that α_{1B}-AR/α_{1D}-AR dimerization facilitates quantitative translocation of α_{1D}-ARs to the cell surface.

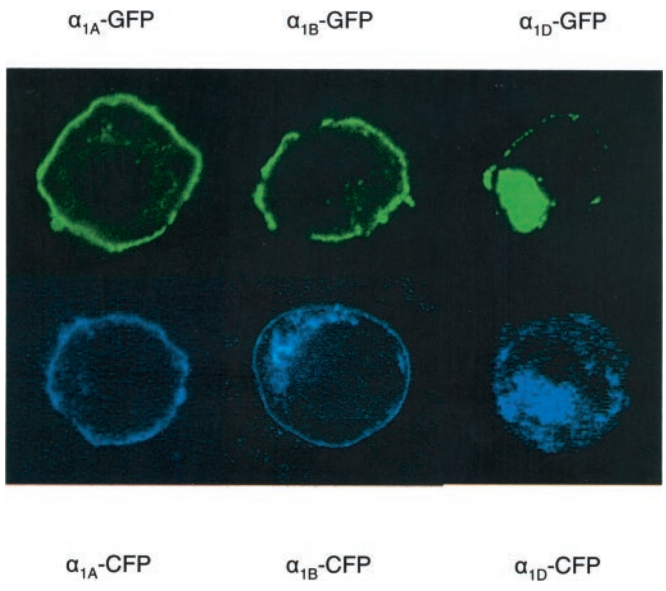

FIG. 1. **Cellular localization of α_1-AR subtypes.** HEK293 cells were transiently transfected with C-terminal GFP-tagged (*upper*) or C-terminal CFP-tagged (*lower*) α_1-AR subtypes. Cells were visualized using laser confocal microscopy according to the protocol detailed under "Experimental Procedures." Each *image* is representative of the large majority of cells observed from several individual experiments (Table I).

Co-expression of α_{1A}-/α_{1D}-ARs Does Not Result in Surface Localization of α_{1D}-ARs—Our previous data showed that epitope-tagged α_{1A}- and α_{1D}-ARs do not form heterodimers (39). Therefore, we hypothesized that co-expression of α_{1A}- and α_{1D}-ARs would not result in differences in cellular localization of either α_1-AR subtype. Using the same protocol used in α_{1B}-/α_{1D}-AR co-transfections, HEK293 cells were co-transfected with GFP-tagged α_{1D}-ARs and HA-tagged α_{1A}-ARs, or with GFP-tagged α_{1A}-ARs and CFP-tagged α_{1D}-ARs. As shown in Fig. 2*B*, confocal imaging revealed that co-transfection of α_{1A}- and α_{1D}-ARs resulted in a primarily intracellular localization of α_{1D}-ARs, whereas α_{1A}-ARs were almost exclusively found on the plasma membrane. These results were again supported using the luminometer-based cell surface assay to compare expression of FLAG-tagged α_{1D}-ARs expressed alone or in combination with HA-tagged α_{1A}-ARs (Fig. 2*C*). Unlike co-expression with α_{1B}-ARs, co-expression with α_{1A}-ARs resulted in no significant increase in surface expression of α_{1D}-ARs, in comparison to transient expression of FLAG-α_{1D}-ARs alone. Therefore, these data suggest that co-expression of α_{1A}- and α_{1D}-ARs does not alter the cellular localization of α_{1D}-ARs.

Role of the α_{1B}-AR N- and C-terminal Domains in Heterodimerization—Previous work using N- and C-terminal truncation constructs has indicated that α_{1B}-AR homo- and heterodimerization does not involve either the N or C terminus (37, 39). To determine if these domains are necessary for the ability of α_{1B}-ARs to promote α_{1D}-AR trafficking to the plasma membrane, we co-transfected HEK293 cells with HA-tagged α_{1B}-ARs truncated at either the N terminus ($\Delta^{1-38}\alpha_{1B}$) or C terminus ($\Delta^{366-519}\alpha_{1B}$) (Fig. 3*A*) in addition to GFP-tagged α_{1D}-ARs. Confocal imaging of transfected cells revealed that both N- and C-truncated forms of the α_{1B}-AR were fully capable of trafficking GFP-tagged α_{1D}-ARs to the plasma membrane (Fig. 3*B*). Using the cell surface assay to confirm these results, we found that both truncated forms of the α_{1B}-AR were not significantly different from wild-type α_{1B}-ARs in their abilities to promote surface expression of FLAG-α_{1D}-ARs (Fig. 3*C*). Therefore, these data show that the α_{1B}-AR N- and C-terminal domains are not necessary for trafficking α_{1D}-ARs to the plasma membrane and suggest that the α_{1B}-AR hydrophobic core or intracellular/extracellular loops are primarily responsible.

TABLE I

Cellular localization of GFP-tagged α_1-ARs heterologously expressed in HEK293 cells

GFP-tagged α_1-AR subtypes were transiently transfected into HEK293 cells. Fields of cells were examined under a fluorescent microscope. Individual cells were classified as having fluorescence almost exclusively in a bright ring surrounding the cell (*surface*), or dense intracellular fluorescence (*intracellular*). Data are expressed as mean number of cells ± S.E. and represent results from multiple experiments.

Receptor	No. of cells intracellular	No. of cells surface	Total intracellular	Total surface
			%	%
α_{1A}-GFP	16 ± 4	221 ± 25	6.7	93.3
α_{1B}-GFP	37 ± 4	188 ± 23	16.4	83.6
α_{1D}-GFP	201 ± 33	22 ± 6	90.3	9.7
HAα_{1B}/α_{1D}-GFP	102 ± 4	182 ± 35	35.8	64.2

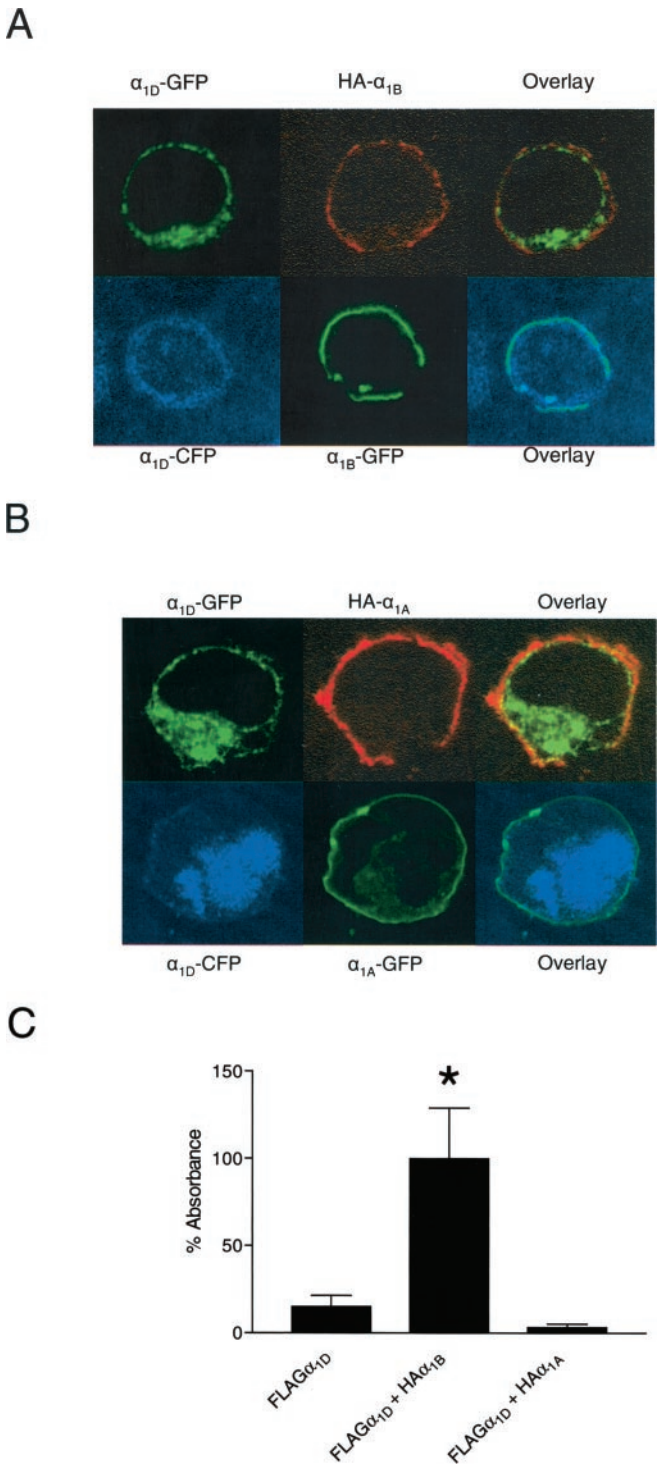

FIG. 2. **Cellular localization of co-expressed α_1-AR subtypes.** HEK293 cells were transiently co-transfected with *A*, N-terminal HA-tagged α_{1B}- and C-terminal GFP-tagged α_{1D}-ARs (*upper*) or C-terminal GFP-tagged α_{1B}- and C-terminal CFP-tagged α_{1D}-ARs (*lower*) or *B*, N-terminal HA-tagged α_{1A}-AR and C-terminal GFP-tagged α_{1D}-ARs (*upper*) or C-terminal GFP-tagged α_{1A}-AR and C-terminal CFP-tagged α_{1D}-ARs (*lower*). Cells were visualized using laser confocal microscopy according to the protocol detailed under "Experimental Procedures." Each *image* is representative of many cells from two to three individual experiments. *C*, cell surface expression of FLAG-tagged α_{1D}-ARs was detected using a luminometer-based assay after transient co-transfection with HA-tagged α_{1A}- or α_{1B}-ARs, as described under "Experimental Procedures." The values for each experiment are represented as percent absorbance, with 100% absorbance equal to the average observed with FLAG-tagged α_{1D}-AR co-expressed with HA-tagged α_{1B}-AR. The data are expressed as mean ± S.E. of four independent experiments (*, significantly different then FLAG-α_{1D}-AR expressed alone, $p < 0.05$).

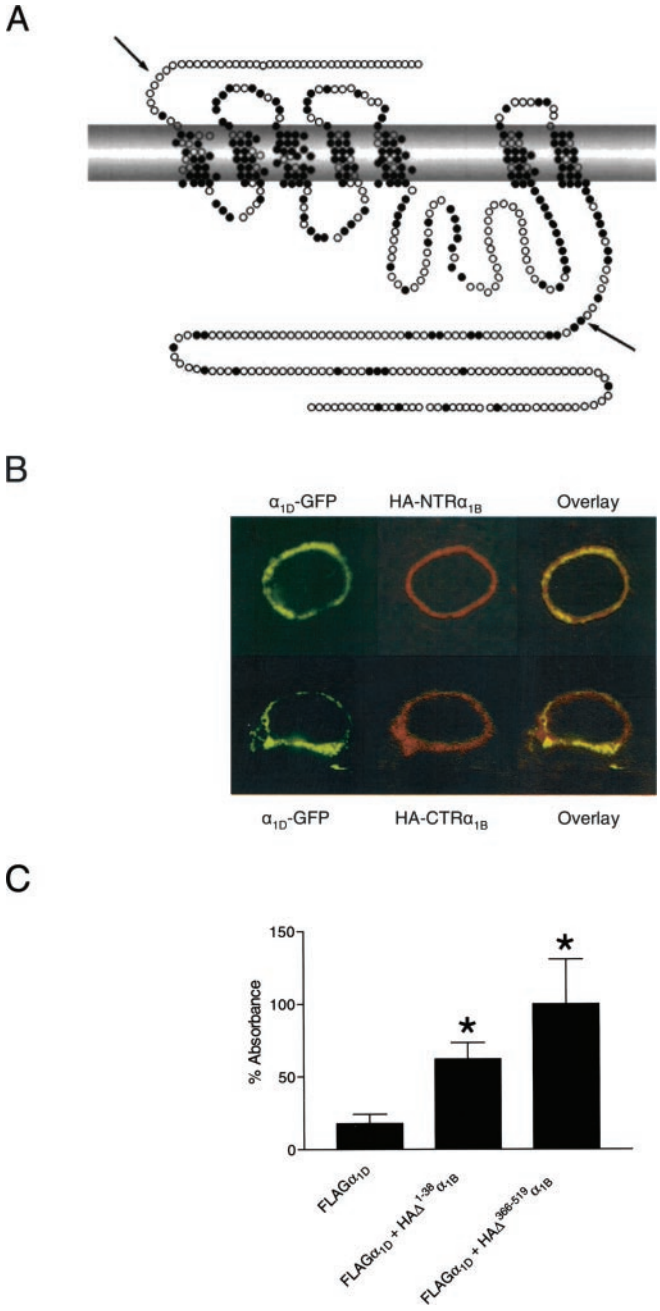

FIG. 3. **Role of the N- and C-terminal domains of α_{1B}-ARs in translocation of α_{1D}-ARs to the cell surface.** *A*, sequence comparison of human α_{1A}- and α_{1B}-ARs. The α_{1B}-AR backbone is used for comparison. Amino acid residues identical in the two subtypes are shown as *closed circles*, whereas variable amino acids are shown as *open circles*. *Arrows* indicate N-terminal and C-terminal truncations. *B*, HEK293 cells were transiently co-transfected with C-terminal GFP-tagged α_{1D}-ARs and HA-tagged $\Delta^{1-38}\alpha_{1B}$-ARs (*upper*) or HA-tagged $\Delta^{366-519}\alpha_{1B}$-ARs (*lower*). Cells were visualized using laser confocal microscopy as detailed under "Experimental Procedures." Each *image* is representative of many cells from two to three individual experiments. *C*, cell surface expression of N-terminal FLAG-tagged α_{1D}-ARs was determined upon co-expression with either HA-tagged $\Delta^{1-38}\alpha_{1B}$- or $\Delta^{366-519}\alpha_{1B}$-ARs using a luminometer-based assay as described under "Experimental Procedures." The values for each experiment are represented as percent absorbance, with 100% absorbance equal to the average observed with FLAG-tagged α_{1D}-ARs co-expressed with HA-tagged $\Delta^{366-519}\alpha_{1B}$-ARs. The data are expressed as mean ± S.E. of four independent experiments (*, significantly different than FLAG-α_{1D}-ARs expressed alone, $p < 0.05$).

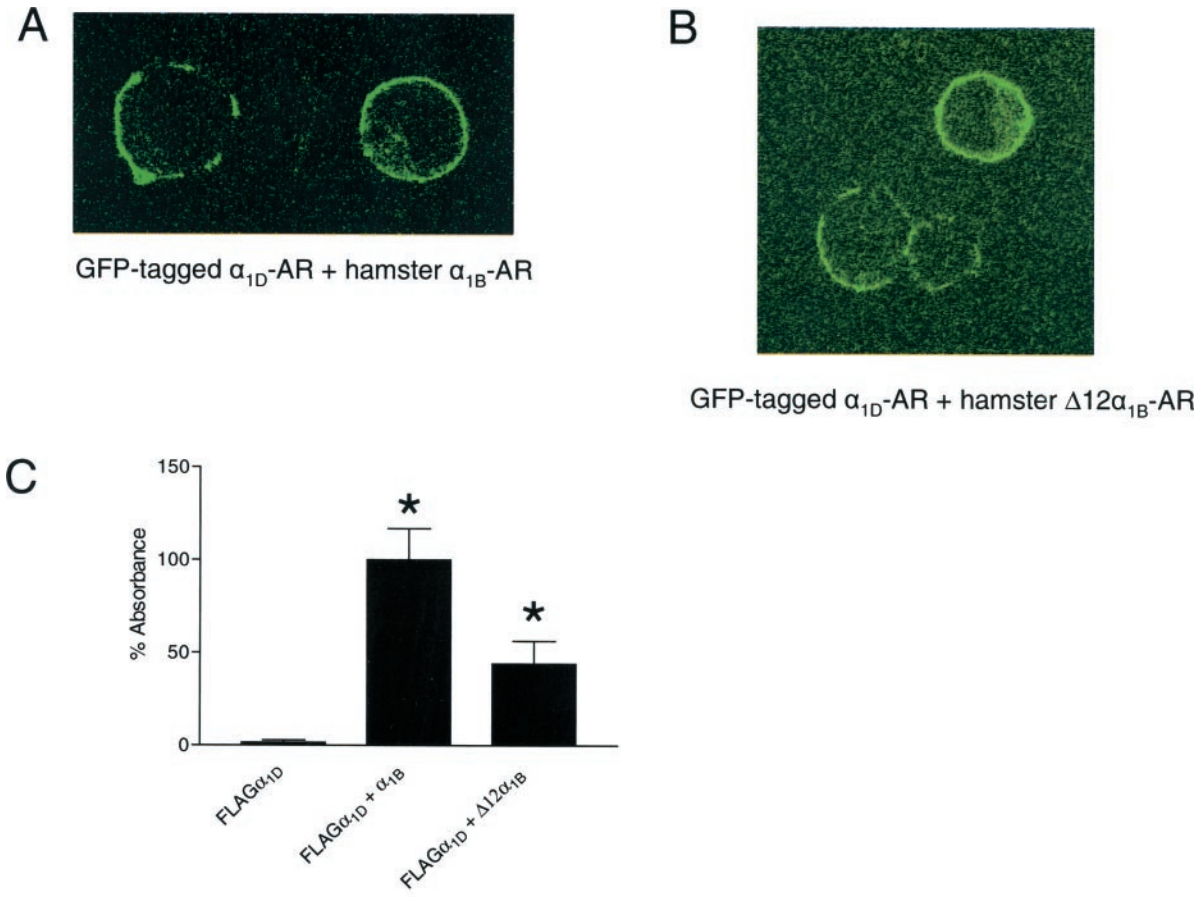

FIG. 4. **Hamster full-length and $\Delta12\alpha_{1B}$-ARs traffic α_{1D}-ARs to the cell surface.** HEK293 cells were transiently co-transfected with C-terminal GFP-tagged α_{1D}-ARs and *A*, full-length hamster α_{1B}-ARs or *B*, untagged $\Delta12\alpha_{1B}$-ARs. Cells were visualized using laser confocal microscopy as detailed under "Experimental Procedures." Each *image* is representative of many cells from two individual experiments. *C*, cell surface expression of N-terminal FLAG-tagged α_{1D}-ARs was determined upon co-expression with full-length hamster α_{1B}-or hamster $\Delta12\alpha_{1B}$-ARs using a luminometer-based assay as described under "Experimental Procedures." The values for each experiment are represented as percent absorbance, with 100% absorbance equal to the average observed with FLAG-tagged α_{1D}-ARs co-expressed with full-length hamster α_{1B}-ARs. The data are expressed as mean ± S.E. of four independent experiments (*, significantly different then FLAG-α_{1D}-ARs expressed alone, $p < 0.05$).

Role of α_{1B}-/α_{1D}-AR Heterodimerization in α_{1D}-AR Coupling to Functional Responses—Of the three α_1-AR subtypes, α_{1D}-ARs are least efficiently coupled to functional responses in transfected cells (16). Because we found that α_{1B}-/α_{1D}-AR dimerization increases α_{1D}-AR surface expression, we hypothesized that α_{1D}-AR coupling to functional responses might be increased when co-transfected with α_{1B}-ARs. However, because all three α_1-ARs are G_q-coupled receptors and there are few selective antagonists that can effectively distinguish between α_{1B}- and α_{1D}-ARs, it is difficult to pharmacologically isolate the relative contributions of individual subtypes in stimulating functional responses when they are co-expressed. To address this problem, we used a hamster α_{1B}-AR containing a 3-amino acid deletion at residues 227–229 ($\Delta12\alpha_{1B}$-AR), which has previously been reported to be completely uncoupled from all functional responses (46–48). We found that both full-length and $\Delta12$ hamster α_{1B}-ARs were capable of promoting α_{1D}-AR surface expression in HEK293 cells, as evidenced by confocal imaging of GFP-tagged α_{1D}-ARs (Fig. 4, *A* and *B*) and luminometer cell surface detection of FLAG-α_{1D}-ARs (Fig. 4*C*). This enabled us to drive α_{1D}-AR surface expression using an uncoupled α_{1B}-AR, while simultaneously allowing us to measure α_{1D}-AR functional responsiveness in the absence of responses mediated by α_{1B}-ARs. To determine the effect of $\Delta12\alpha_{1B}$-AR co-transfection on α_{1D}-AR coupling to functional responses, we measured NE-stimulated intracellular Ca^{2+} mobilization and [^{3}H]InsP formation in transiently transfected HEK293 cells. As shown in Figs. 5 and 6, NE stimulation of FLAG-α_{1D}-ARs resulted in only minor increases in [^{3}H]InsP formation and intracellular Ca^{2+} mobilization in comparison to HA-α_{1B}-ARs, which generated much larger increases in both responses upon NE stimulation. In agreement with previous studies suggesting hamster $\Delta12\alpha_{1B}$-ARs are uncoupled to functional responses, NE was unable to stimulate [^{3}H]InsP formation or mobilize intracellular Ca^{2+} in HEK293 cells expressing hamster $\Delta12\alpha_{1B}$-ARs alone. Interestingly, co-transfection of FLAG-α_{1D}- and hamster $\Delta12\alpha_{1B}$-ARs increased the level of NE-stimulated Ca^{2+} mobilization to 41 ± 3.1% of the 100 μM UTP response (Fig. 5), similar to the level of Ca^{2+} mobilization induced by NE-stimulation of wild type α_{1B}-ARs (42 ± 16.8%). In contrast, co-transfection of FLAG-α_{1D}- and $\Delta12\alpha_{1B}$-ARs resulted in no significant increase in NE-stimulated [^{3}H]InsP formation (Fig. 6) relative to that observed in HEK293 cells expressing FLAG-tagged α_{1D}-ARs alone. These data suggest that α_{1B}-AR-induced translocation of α_{1D}-ARs to the cell surface results in increased coupling to NE-stimulated Ca^{2+} mobilization but does not increase coupling to NE-stimulated [^{3}H]InsP formation under the conditions of our assays.

α_{1D}-ARs Are Internalized upon Agonist Stimulation—One possible explanation of the differential effects of co-expression with α_{1B}-ARs on α_{1D}-AR-stimulated Ca^{2+} mobilization and [^{3}H]InsP formation is the duration of agonist stimulation in the two assays. Intracellular Ca^{2+} mobilization is measured within seconds of adding agonist, whereas [^{3}H]InsP formation assay is

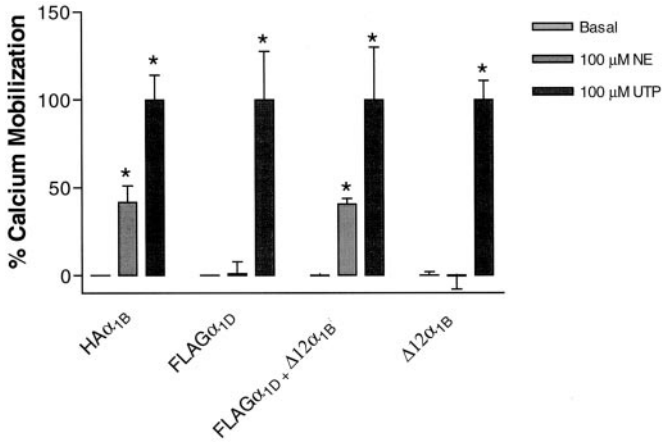

FIG. 5. **Co-expression with hamster $\Delta12\alpha_{1B}$-ARs enhances α_{1D}-AR coupling to intracellular Ca^{2+} mobilization.** HEK293 cells were transiently co-transfected with α_1-ARs and loaded with fura-2. Cells were stimulated with 100 μM NE or 100 μM UTP as described under "Experimental Procedures," and $[Ca^{2+}]_i$ was measured. The values for each experiment are represented as percent Ca^{2+} mobilization, with 100% mobilization equal to the average stimulated by 100 μM UTP in HEK293 cells expressing HA-tagged α_{1B}-ARs. The data are expressed as mean ± S.E. of data from three to four separate experiments (*, significantly different then basal, $p < 0.05$).

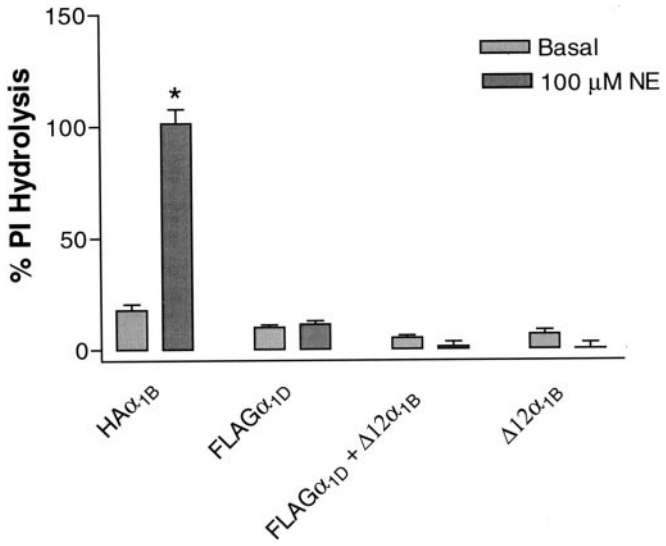

FIG. 6. **Co-expression with hamster $\Delta12\alpha_{1B}$-ARs does not enhance α_{1D}-AR coupling to inositol phosphate formation.** HEK293 cells were transiently co-transfected with α_1-ARs and prelabeled with 1 μCi *myo*-[^{3}H]inositol for 24 h. Cells were stimulated with 100 μM NE for 1 h, and [^{3}H]InsPs were isolated as described under "Experimental Procedures." The values for each experiment are represented as percent hydrolysis, with 100% hydrolysis equal to the level of NE-stimulated hydrolysis in HEK293 cells expressing HA-tagged α_{1B}-ARs. The data are expressed as mean ± S.E. of data from three separate experiments performed in duplicate or triplicate (*, significantly different then basal, $p < 0.05$).

measured after 1 h of agonist stimulation. Therefore, we hypothesized that the lack of increase in NE-stimulated [^{3}H]InsP formation in cells co-expressing α_{1B}- and α_{1D}-ARs might potentially be due to agonist-induced internalization of α_{1D}-ARs. Previous reports have shown that α_{1B}-ARs are rapidly internalized upon agonist stimulation (47). However, there are no previous reports investigating α_{1D}-AR internalization, because this receptor is almost exclusively intracellular after heterologous expression. To measure α_{1D}-AR internalization, HEK293 cells transiently expressing α_1-ARs were stimulated for 1 h with 100 μM NE, and the amount of α_1-AR surface expression

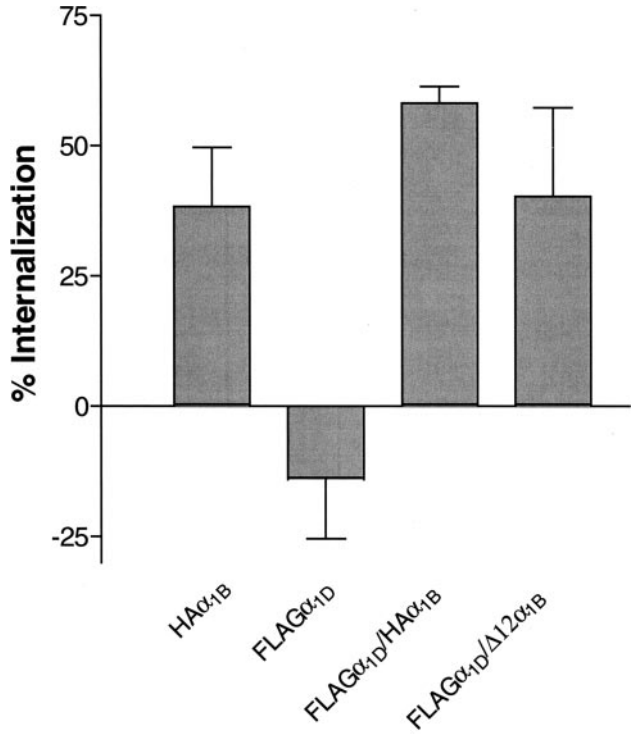

FIG. 7. **α_{1D}-ARs are internalized upon agonist stimulation.** HEK293 cells were transiently transfected with α_1-ARs and cell surface expression of HA-tagged α_{1B}-ARs (*left bar*) or FLAG-tagged α_{1D}-ARs (*right three bars*) was determined using a luminometer-based assay as described under "Experimental Procedures." Cells treated with 100 μM NE were stimulated for 1 h. The values for each experiment are represented as percent internalization from the cell surface. The data are expressed as mean ± S.E. from data from three to four separate experiments (*, significantly different then basal, $p < 0.05$).

was determined using the luminometer-based cell surface assay (Fig. 7). As reported in previous studies (49, 50), HA-tagged α_{1B}-AR cell surface expression decreased (38 ± 11.4%) after treatment with 100 μM NE for 1 h, whereas surface expression of FLAG-tagged α_{1D}-ARs expressed alone was low and unchanged by NE treatment. As described above, α_{1D}-AR cell surface expression was robustly increased upon co-expression with either α_{1B}- or hamster $\Delta12\alpha_{1B}$-ARs. Interestingly, stimulation with 100 μM NE for 1 h decreased FLAG-tagged α_{1D}-AR cell surface expression by 61 ± 3.1% when co-expressed with HA-tagged α_{1B}-ARs and by 46 ± 17.1% when co-expressed with hamster $\Delta12\alpha_{1B}$-ARs. Therefore, these data demonstrate that, when co-expressed with α_{1B}-ARs, α_{1D}-ARs are expressed at the cell surface and undergo profound internalization upon stimulation with agonist.

Cellular Localization of GFP-tagged α_{1D}-ARs Differs between DDT$_1$MF-2 and RASM Cells—The studies performed in HEK293 cells clearly demonstrate that co-expression of α_{1B}-ARs promotes surface expression of α_{1D}-ARs. We wanted to determine if transfecting α_{1D}-ARs into a cell line that endogenously expresses α_{1B}-ARs would result in surface expression of α_{1D}-ARs. DDT$_1$MF-2 cells, a smooth muscle derived cell line from which the hamster α_{1B}-AR was originally cloned (51), express α_{1B}-ARs at a density of ~400 fmol/mg of protein but do not express α_{1A}- or α_{1D}-ARs (52). As shown in Fig. 8*A*, transient transfection of GFP-tagged α_{1D}-ARs into DDT$_1$MF-2 cells resulted almost exclusively in surface localization of α_{1D}-ARs in all cells observed, although slightly more diffuse intracellular signal was seen than was observed with co-transfection of both subtypes in HEK293 cells (Fig. 2). We also examined α_{1D}-AR expression in RASM cells, another smooth muscle-derived cell line that, however, exhibits no endogenous α_1-AR expression

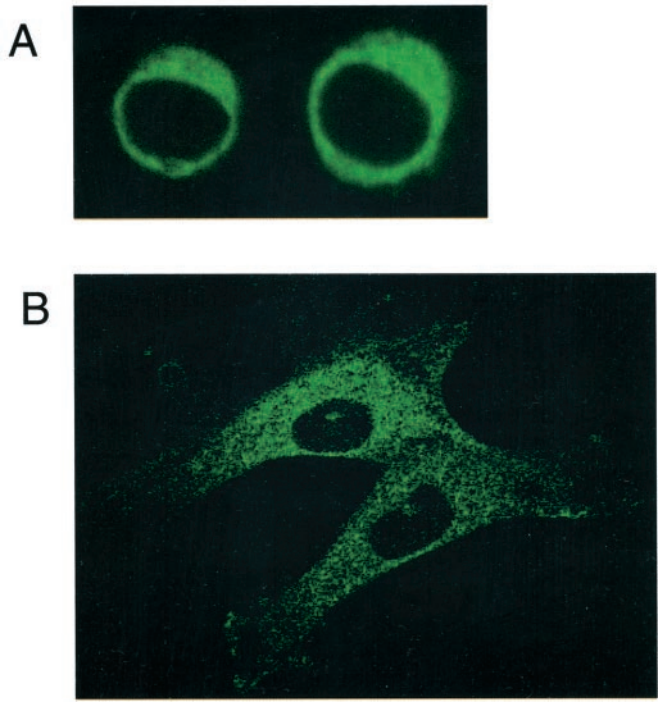

FIG. 8. **GFP-tagged α_{1D}-ARs are located on the cell surface in DDT$_1$MF-2 cells but not in RASMs.** *A*, DDT$_1$MF-2 cells were transiently transfected with C-terminal GFP-tagged α_{1D}-ARs. *B*, RASM cells were retrovirally transfected with C-terminal GFP-tagged α_{1D}-ARs. Cells were visualized using laser confocal microscopy according to the protocol detailed under "Experimental Procedures." Each *image* is representative of all cells observed in two to three separate experiments.

(18). Because RASMs are very difficult to transfect with plasmids, we used a retroviral transfection method. In striking contrast to DDT$_1$MF-2 cells, retroviral transfection of GFP-tagged α_{1D}-ARs into RASM cells resulted in an almost exclusive intracellular localization of the receptor (Fig. 8*B*), similar to that observed in HEK293 cells. These data support the idea that α_{1B}-AR heterodimerization with α_{1D}-ARs results in trafficking of α_{1D}-ARs to the cell surface and suggest that endogenous levels of α_{1B}-ARs in DDT$_1$MF-2 cells are sufficient to mediate a strong cell type-dependent regulation of α_{1D}-AR subcellular localization.

DISCUSSION

The data presented here show that α_{1D}-AR co-expression with α_{1B}-ARs, but not α_{1A}-ARs, results in quantitative surface expression of α_{1D}-ARs, which is almost exclusively intracellular when expressed alone. Since our previous data using co-immunoprecipitation has shown direct interactions of α_{1D}- with α_{1B}-, but not α_{1A}-ARs (39), we believe that the effect of the α_{1B}-AR on α_{1D}-AR surface expression is likely to be due to direct heterodimerization of the two subtypes. This phenomenon appears to involve primarily the α_{1B}-AR hydrophobic core or intracellular/extracellular loops, because N- and C-terminal truncation mutants are as effective as full-length receptors. It does not appear to require α_{1B}-AR G protein coupling or second messenger responses, because it is also observed with functionally uncoupled α_{1B}-ARs. In addition, promotion of surface expression of α_{1D}-ARs by heterodimerization with α_{1B}-ARs is associated with increased α_{1D}-AR responsiveness and internalization. Finally, α_{1D}-AR surface expression also appears to be strongly promoted by natively expressed α_{1B}-ARs in DDT$_1$MF-2 cells, suggesting that it is not an artifact of overexpressed recombinant proteins.

The results presented here are somewhat similar to what has been observed previously with the GABA$_B$ receptor, where GABA$_B$-R1 expressed alone is retained in the endoplasmic reticulum, and co-expression of GABA$_B$-R2 is necessary to transport GABA$_B$R1 to the cell surface and form a functional receptor (34). However, there are several striking differences between the GABA$_B$R findings and our results. First, GABA$_B$ receptors belong to the much smaller Class III family of receptors and exhibit very large extracellular N-terminal domains that contain the agonist binding sites and very large cytoplasmic C termini that contribute to receptor dimerization (22). Second, and more importantly, the individual GABA$_B$ subunits do not form functional receptors when expressed alone, and the heterodimer appears to form only a single receptor (34). In contrast, Class I GPCRs, including α_1-ARs, have agonist binding sites at least partially within the hydrophilic pocket formed by the seven transmembrane domains and clearly form functional receptors with the expected pharmacology when expressed alone. Although we do not yet know whether α_{1B}/α_{1D}-AR heterodimers function as a single receptor, our previous data examining the pharmacology of co-expressed subtypes suggest that each retains its own unique pharmacological characteristics (39), suggesting that they remain independent receptor subtypes.

One of the most surprising findings of our previous work (39), and this study is the subtype selectivity observed. Because α_{1A}- and α_{1B}-ARs share a high degree of sequence homology (Fig. 3*A*), the dramatic differences between these two subtypes in their abilities to translocate α_{1D}-ARs to the cell surface is quite unexpected. Because the domains of these receptors with the least sequence homology are the extracellular N terminus and intracellular C terminus, it was even more surprising to find that these domains are not required for heterodimerization and/or translocation. This is unlike the GABA$_B$ receptors (22, 53) and mGluR1 (54) receptors, which dimerize at least partially through interactions at their C- and N-terminal domains, respectively. Our data are consistent with the idea that α_{1B}-/α_{1D}-AR heterodimerization involves primarily the hydrophobic core of the α_{1B}-AR, an idea that has previously been suggested for other Class I GPCRs, including β_2-ARs (55), dopamine D2 (56), and rhodopsin (57) receptors. Interestingly, the α_{1A}-AR and α_{1B}-AR transmembrane domains differ by only 35 amino acids, which should greatly facilitate identification of particular amino acids or domains involved in dimerization.

Using the uncoupled hamster $\Delta12\alpha_{1B}$-AR mutant, we found that dimerization induced translocation of α_{1D}-ARs to the cell surface, resulting in increased coupling of this receptor to Ca^{2+} mobilization. These results show that α_{1B}-AR coupling is not required for α_{1D}-AR translocation and rule out the role of downstream signaling. These findings may also shed light on differences between the coupling efficiency of heterologously expressed and *in vivo* α_{1D}-ARs. Although heterologously expressed α_{1D}-ARs weakly couple to second messenger responses (16–18), stimulation of α_{1D}-ARs in intact blood vessels is very effective in causing contraction (19–21). Evidence from α_{1B}-AR knockout mice supports the idea that the presence of α_{1B}-AR is important for α_{1D}-AR function *in vivo*, because phenylephrine-induced contraction of aortic rings occurred with lower potency and intrinsic activity in comparison to wild-type animals (7). However, a subsequent report did not confirm this observation (58). Also, phenylephrine stimulates decreases in left ventricular pressure and coronary blood flow in α_{1A}-/α_{1B}-AR double knockout mice (8), suggesting that heterodimerization with α_{1B}-ARs cannot be the only mechanism involved in determining the surface expression of functional α_{1D}-ARs. We are currently examining whether other GPCRs may also promote α_{1D}-AR surface expression, which might explain why α_{1D}-ARs can still function in α_{1B}-AR knockout mice.

Heterodimerization of α_{1D}-ARs with the inactive $\Delta12\alpha_{1B}$-AR mutant resulted in striking increases in agonist-induced Ca^{2+} mobilization, but no significant increase in agonist-induced [^{3}H]InsP formation. The main difference between these assays is the time of agonist exposure, being seconds for Ca^{2+} measurements and 1 h for [^{3}H]InsPs measurements. Therefore, we determined whether the observed difference might be due to rapid α_{1D}-AR desensitization and internalization. Although desensitization has been examined extensively for α_{1B}-ARs (43), there are few reports on α_{1D}-ARs, presumably because of difficulties in obtaining significant expression levels in heterologous systems. However, one report (59) has suggested that α_{1D}-ARs are rapidly phosphorylated (~1 min) upon stimulation with NE or treatment with phorbol esters, resulting in rapid desensitization. We found that 1-h stimulation with NE reduced surface FLAG-α_{1D}-AR expression (co-expressed with α_{1B}-ARs) by >60%. These data support the idea that the lack of α_{1D}-AR induced [^{3}H]InsP formation may be a result of rapid α_{1D}-AR desensitization/internalization.

Increasing interest in the cellular localization of GPCRs has been spurred by identification of diseases caused by protein mislocalization, including hypercholesterolemia, cystic fibrosis, and nephrogenic diabetes insipidus (60). Although GPCRs are usually assumed to be expressed primarily on the cell surface when heterologously expressed, this is not always the case. In fact, many GPCRs are found primarily in intracellular compartments after heterologous expression, including α_{1D}-ARs (13, 18), α_{2C}-ARs (61–63), $GABA_BR1$ (34), adenosine-2b (64), sweet taste (35), bitter taste (65), and the large family of odorant (66) receptors, as well as ion channel receptors, including the 5-$HT3_B$ subtype (67). These receptors are often found retained in the endoplasmic reticulum, where they are unlikely to respond to agonist stimulation. The mechanisms involved in intracellular retention of receptors remain unclear in most cases. Some GPCRs contain ER retention motifs that must be removed or masked before they can be exported, including the CB1 N terminus (68) and $GABA_B$-R1 C terminus (34). Other GPCRs may be targeted by ER retention proteins such as HSP79 analogue BiP/GRP78 (69) or the lectin-like proteins calnexin and calreticulin (70, 71), preventing surface expression. We show here that α_{1B}-ARs promote α_{1D}-AR surface expression, presumably by direct heterodimerization. Previously, we showed that N-terminal truncation promotes surface expression of α_{1D}-ARs through a transplantable sequence contained within the relatively long N terminus (17, 18). Thus, α_{1B}-AR/α_{1D}-AR heterodimerization may mask an ER retention signal in the α_{1D}-AR N terminus, although this hypothesis remains to be tested.

Although these results suggest a clear functional role for α_1-AR heterodimerization, there are a number of caveats. Because of the lack of specific antibodies, only recombinant tagged receptors were examined. However, many previous studies have shown that epitope-tagged α_1-ARs are pharmacologically and functionally equivalent to wild type receptors, and we also minimized this issue with combinations of different C-terminal and N-terminal tags. Another potential limitation is our primary use of HEK293 cells as a convenient model, and possible receptor overexpression. However, we also transfected GFP-tagged α_{1D}-ARs into a hamster smooth muscle cell line (DDT_1MF-2), which endogenously expresses α_{1B}-ARs, as well as a rat aorta smooth muscle cell line that expresses no detectable ARs. Because GFP-tagged α_{1D}-ARs were expressed on the cell surface in DDT_1MF-2 cells, this suggests that wild-type α_{1B}-ARs can also promote α_{1D}-AR surface expression at physiologically relevant levels. This is in direct contrast to RASMs, where GFP-tagged α_{1D}-ARs are primarily intracellular, just as in HEK293 (13, 18), COS (14), and CHO (18) cells.

These data provide clear evidence for a dramatic functional role of subtype-specific heterodimerization of α_1-ARs. Despite the growing list of receptors that undergo homo- and heterodimerization (22–34), dimerization of Class I GPCRs has usually been found to be associated with only small differences in receptor pharmacology, function, or agonist-induced internalization. This study expands this list to a major role in receptor trafficking to the plasma membrane, similar to that observed previously with the Class III $GABA_B$ receptors, where two subunits are required for surface expression. It will be interesting in future studies to determine whether heterodimers of Class I receptors, like the α_{1B}/α_{1D}-AR heterodimer described here, remain together on the cell surface, and if so, whether they function as one (like the $GABA_B$) or two distinct receptors. In any case, these studies contribute to a growing recognition of the importance of dimerization in GPCR pharmacology and function.

Acknowledgments—We thank Dr. Howard Rees and Dr. Alan Levey for help with confocal microscope experiments and Dr. Steven Prinster and Dr. Myron Toews for helpful discussions.

REFERENCES

1. Bockaert, J., and Pin, J.-P. (1999) *EMBO J.* **18,** 1723–1729
2. Zhong, H., and Minneman, K. P. (1999) *Eur. J. Pharmacol.* **375,** 261–276
3. Hague, C., Uberti, M., Chen, Z. J., and Minneman, K. P. (2003) *Life Sci.* **74,** 411–418
4. Piascik, M. T., and Perez, D. M. (2001) *J. Pharmacol. Exp. Ther.* **298,** 403–410
5. Rokosh, D. G., and Simpson P. C. (2002) *Proc. Natl. Acad. Sci. U. S. A.* **99,** 9474–9479
6. Tanoue, A., Nasa, Y., Koshimizu, T., Shinoura, H., Oshikawa, S., Kawai, T., Sunada, S., Takeo, S., and Tsujimoto, G. (2002) *J. Clin. Invest.* **109,** 765–775
7. Cavalli, A., Lattion, A. L., Hummler, E., Nenniger, M., Pedrazzini, T., Aubert, J. F., Michel, M. C., Yang, M., Lembo, G., Vecchione, C., Mostardini, M., Schmidt, A., Beermann, F., and Cotecchia S. (1997) *Proc. Natl. Acad. Sci. U. S. A.* **94,** 11589–11594
8. Turnbull, L., McCloskey, D., O'Connell, T., Simpson, P., and Baker, A. (2003) *Am. J. Physiol.* **284,** H1104–H1109
9. Gonzalez-Cabrera, P. J., Gaivin, R. J., Yun, J., Ross, S. A., Papay, R. S., McCune, D. F., Rorabaugh, B. R., and Perez, D. M. (2003) *Mol. Pharmacol.* **63,** 1104–1116
10. Chen, S., Lin, F., Iismaa, S., Lee, K. N., Birckbichler, P. J., and Graham, R. M. (1996) *J. Biol. Chem.* **271,** 32385–32391
11. Diviani, D., Lattion, A. L., Abuin, L., Staub, O., and Cotecchia S. (2003) *J. Biol. Chem.* **278,** 19331–19340
12. Xu, Z., Hirasawa, A., Shinoura, H., and Tsujimoto, G. (1999) *J. Biol. Chem.* **274,** 21149–21154
13. Chalothorn, D., McCune, D. F., Edelmann, S. E., Garcia-Cazarin, M. L., Tsujimoto, G., and Piascik, M. T. (2002) *Mol. Pharmacol.* **61,** 1008–1016
14. Hirasawa, A., Sugawara, T., Awaji, T., Tsumaya, K., Ito, H., and Tsujimoto, G. (1997) *Mol. Pharmacol.* **52,** 764–770
15. Mackenzie, J. F., Daly, C. J., Pediani, J. D., and McGrath, J. C. (2000) *J. Pharmacol. Exp. Ther.* **294,** 434–443
16. Theroux, T. L., Esbenshade, T. A., Peavy, R. D., and Minneman, K. P. (1996) *Mol. Pharmacol.* **50,** 1376–1387
17. Pupo, A. S., Uberti, M. A., and Minneman, K. P. (2003) *Eur. J. Pharmacol.* **462,** 1–8
18. Hague, C., Chen, Z., Pupo, A. S., Schulte, N. A., Toews, M. L., and Minneman, K. P. (2004) *J. Pharmacol. Exp. Ther.* **309,** 1–10
19. Piascik, M. T., Guarino, R. D., Smith, M. S., Soltis, E. E., Saussy, D. L., Jr., and Perez, D. M. (1995) *J. Pharmacol. Exp. Ther.* **275,** 1583–1589
20. Hussain, M. B., and Marshall, I. (2000) *Eur. J. Pharmacol.* **395,** 69–76
21. Hussain, M. B., and Marshall, I. (1997) *Br. J. Pharmacol.* **122,** 849–858
22. Bouvier, M. (2001) *Nat. Rev. Neurosci.* **2,** 274–286
23. Heldin, C. H., (1995) *Cell* **80,** 213–223
24. Rios, C. D., Jordan, B. A., Gomes, I., and Devi, L. A. (2001) *Pharmacol. Ther.* **92,** 71–87
25. Cvejic, S., and Devi, L. A. (1997) *J. Biol. Chem.* **272,** 26959–26964
26. Karpa, K. D., Lin, R., Kabbani, N., and Levenson, R. (2000) *Mol. Pharmacol.* **58,** 677–683
27. Bai, M., Trivedi, S., and Brown, E. M. (1998) *J. Biol. Chem.* **273,** 23605–23610
28. Lavoie, C., Mercier, J. F., Salahpour, A., Umapathy, D., Breit, A., Villeneuve, L. R., Zhu, W. Z., Xiao, R. P., Lakatta, E. G., Bouvier, M., and Hebert, T. E. (2002) *J. Biol. Chem.* **277,** 35402–35410
29. George, S. R., Fan, T., Xie, Z., Tse, R., Tam, V., Varghese, G., and O'Dowd, B. F. (2000) *J. Biol. Chem.* **275,** 26128–26135
30. Jordan, B. A., and Devi, L. A., (1999) *Nature* **399,** 697–700
31. Xie, Z., Lee, S. P., O'Dowd, B. F., and George, S. R. (1999) *FEBS Lett.* **456,** 63–67
32. Xu, J., He, J., Castleberry, A. M., Balasubramanian, S., Lau, A. G., and Hall, R. A. (2003) *J. Biol. Chem.* **278,** 10770–10770
33. Jordan, B. A., Trapaidze, N., Gomes, I., Nivarthi, R., and Devi, L. A. (2001) *Proc. Natl. Acad. Sci. U. S. A.* **98,** 343–348
34. Margeta-Mitrovic, M., Jan, Y. N., and Jan, L. Y. (2001) *Proc. Natl. Acad. Sci.*

U. S. A. **98,** 14649–14654
35. Nelson, G., Hoon, M. A., Chandrashekar, J., Zhang, Y., Ryba, N. J., and Zuker, C. S. (2001) *Cell* **106,** 381–390
36. Vicentic, A., Robeva, A., Rogge, G., Uberti, M., and Minneman, K. P. (2002) *J. Pharmacol. Exp. Ther.* **302,** 58–65
37. Stanasila, L., Perez, J. B., Vogel, H., and Cotecchia, S. (2003) *J. Biol. Chem.* **278,** 40239–40251
38. Carrillo, J. J., Pediani, J., and Milligan, G. (2003) *J. Biol. Chem.* **278,** 42578–42587
39. Uberti, M. A., Hall, R. A., and Minneman, K. P. (2003) *Mol. Pharmacol.* **64,** 1379–1390
40. Hirasawa, A., Horie, K., Tanaka, T., Takagaki, K., Murai, M., Yano, J., and Tsujimoto, G. (1993) *Biochem. Biophys. Res. Commun.* **195,** 902–909
41. Ramarao, C. S., Denker, J. M., Perez, D. M., Gaiven, R. J., Riek, R. P., and Graham, R. M. (1992) *J. Biol. Chem.* **267,** 21936–21945
42. Esbenshade, T. A., Hirasawa, A., Tsujimoto, G., Tanaka, T., Yano, J., and Minneman, K. P. (1995) *Mol. Pharmacol.* **47,** 977–985
43. Abbott, K. L., Robida, A. M., Davis, M. E., Pavlath, G. K., Camden, J. M., Turner, J. T., and Murphy, T. J. (2000) *J. Mol. Cell Cardiol.* **32,** 391–403
44. Volpicelli, L. A., Lah, J. J., and Levey, A. I. (2001) *J. Biol. Chem.* **276,** 47590–47598
45. Wilson, K. M., Gilchrist, S., and Minneman, K. P. (1990) *J. Neurochem.* **55,** 691–697
46. Wu, D., Jiang, H., and Simon, M. I. (1995) *J. Biol. Chem.* **270,** 9828–9832
47. Toews, M. L., Prinster, S. C., and Schulte, N. A. (2003) *Life Sci.* **74,** 379–389
48. Wang, J., Wang, L., Anderson, J. L., Schulte, N. A., and Toews, M. L. (2002) *J. Pharmacol. Exp. Ther.* **300,** 134–141
49. Zhu, J., Cerutis, D. R., Anderson, J. L., and Toews, M. L. (1996) *Eur. J. Pharmacol.* **299,** 205–212
50. Wang, J., Wang, L., Zheng, J., Anderson, J. L., and Toews, M. L. (2000) *Mol. Pharmacol.* **57,** 687–694
51. Cotecchia, S., Schwinn, D. A., Randall, R. R., Lefkowitz, R. J., Caron, M. G., and Kobilka, B. K. (1988) *Proc. Natl. Acad. Sci. U. S. A.* **85,** 7159–7163
52. Han, C., Esbenshade, T. A., and Minneman, K. P. (1992) *Eur. J. Pharmacol.* **226,** 141–148
53. Kuner, R., Kohr, G., Grunewald, S., Eisenhardt, G., Bach, A., and Kornau, H. C. (1999) *Science* **283,** 74–77
54. Kunishima, N., Shimada, Y., Tsuji, Y., Sato, T., Yamamoto, M., Kumasaka, T., Nakanishi, S., Jingami, H., and Morikawa, K. (2000) *Nature* **407,** 971–977
55. Hebert, T. E., Moffett, S., Morello, J. P., Loisel, T. P., Bichet, D. G., Barret, C., and Bouvier, M. (1996) *J. Biol. Chem.* **271,** 16384–16392
56. Guo, W., Shi, L., and Javitch, J. A. (2003) *J. Biol. Chem.* **278,** 4385–4388
57. Liang, Y., Fotiadis, D., Filipek, S., Saperstein, D. A., Palczewski, K., and Engel, A. (2003) *J. Biol. Chem.* **278,** 21655–21662
58. Daly, C. J., Deighan, C., McGee, A., Mennie, D., Ali, Z., McBridge, M., and McGrath, J. C. (2002) *Physiol. Genomics* **9,** 85–91
59. Garcia-Sainz, J. A., Cuevas-Vazquez, F. G., and Romero-Avila, M. T. (2001) *Biochem. J.* **353,** 603–610
60. Edwards, S. W., Tan, C. M., and Limbird, L. E. (2000) *Trends Pharmacol. Sci.* **21,** 304–308
61. Wozniak, M., and Limbird, L. E. (1996) *J. Biol. Chem.* **271,** 5017–5024
62. Von Zastrow, M., Link, R., Daunt, D., Barsh, G., and Kobilka, B. (1993) *J. Biol. Chem.* **268,** 763–766
63. Daunt, D. A., Hurt, C., Hein, L., Kallio, J., Feng, F., and Kobilka, B. (1997) *Mol. Pharmacol.* **51,** 711–720
64. Sitaraman, S. V., Wang, L., Wong, M., Bruewer, M., Hobert, M., Yun, C. H., Merlin, D., and Madara J. L. (2002) *J. Biol. Chem.* **277,** 33188–33195
65. Chandrashekra, J., Mueller, K., Moon, E., Adler, E., Feng, L., Guo, W., Zuker, C., and Ryba, N. (2000) *Cell* **100,** 703–711
66. Buck, L. B. (2000) *Cell* **100,** 611–618
67. Boyd, G. W., Doward, A. I., Kirkness, E. F., Millar, N. S., and Connolly, C. N. (2003) *J. Biol. Chem.* **278,** 27681–27687
68. Andersson, H., D'Antona, A. M., Kendall, D. A., Von Heijne, G., and Chin, C. N. (2003) *Mol. Pharmacol.* **64,** 570–577
69. Hurtley, S. M., Bole, D. G., Hoover-Litty, H., Helenius, A., and Copeland, C. S. (1989) *J. Cell Biol.* **108,** 2117–2126
70. Kapoor, M., Srinivas, H., Eaazhisai, K., Gemma, E., Ellgaard, L., Oscarson, S., Helenius, A., and Surolia, A. (2003) *J. Biol. Chem.* **278,** 6194–6200
71. Zhang, J. X., Braakman, I., Matlack, K. E., and Helenius, A. (1997) *Mol. Biol. Cell* **8,** 1943–1954